SiliconPV: April 03-05, 2012, Leuven, Belgium

Comparison of ICP-AlO$_x$ and ALD-Al$_2$O$_3$ layers for the rear surface passivation of c-Si Solar cells

B. Veith[a]*, T. Dullweber[a], M. Siebert[a], C. Kranz[a], F. Werner[a], N.-P. Harder[a,b], J. Schmidt[a,c], B.F.P. Roos[d], T. Dippell[d], R. Brendel[a,c]

[a]*Institute for Solar Energy Research Hamelin (ISFH), Am Ohrberg 1, 31860 Emmerthal, Germany*
[b]*Institut für Materialien und Bauelemente der Elektronik, University of Hannover, Schneiderberg 32, 30167 Hannover, Germany*
[c]*Institute of Solid-State Physics, University of Hannover, Appelstrasse 2, 30167 Hannover, Germany*
[d]*Singulus Technologies AG, Hanauer Landstrasse 103, 63796 Kahl am Main, Germany*

Abstract

The deposition rate of the standard (i.e. sequential) atomic layer deposition (ALD) process is very low compared to the plasma-enhanced chemical vapour deposition (PECVD) process. Therefore, as a short- and medium-term perspective, PECVD aluminium oxide (AlO$_x$) films might be better suited for the implementation into industrial-type solar cells than ALD-Al$_2$O$_3$ films. In this paper, we report results achieved with a newly developed PECVD deposition process for AlO$_x$ using an inductively coupled plasma (ICP). We compare the results to high-quality ALD-Al$_2$O$_3$ films. We examine a stack consisting of a thin AlO$_x$ passivation layer and a PECVD silicon nitride (SiN$_y$) capping layer. Surface recombination velocities below 9 cm/s were measured on low-resistivity (1.4 Ωcm) p-type crystalline silicon wafers passivated either by ICP-PECVD-AlO$_x$ films or by ALD-Al$_2$O$_3$ films after annealing at 425°C. Both passivation schemes provide an excellent thermal stability during firing at 910°C with SRVs below 12 cm/s for both, Al$_2$O$_3$/SiN$_y$ stacks and single Al$_2$O$_3$ layers. A fixed negative charge of -4×10^{12} cm^{-2} is measured for ICP-AlO$_x$ and ALD-Al$_2$O$_3$, whereas the interface state density is higher for the ICP-AlO$_x$ layer with values of 11.0×10^{11} eV^{-1}cm^{-2} compared to 1.3×10^{11} eV^{-1}cm^{-2} for ALD-Al$_2$O$_3$. Implemented into large-area screen-printed PERC solar cells, an independently confirmed efficiency of 20.1% for ICP-AlO$_x$ and an efficiency of 19.6% for ALD-Al$_2$O$_3$ are achieved.

Keywords: Silicon; Surface passivation; Aluminum oxide; Solar Cells

* Corresponding author. Tel.: +49-5151-999-635; fax: +49-5151-999-400
E-mail address: veith@isfh.de

1. Introduction

One option for next-generation industrial-type solar cells are passivated emitter and rear solar cells (PERC). For the implementation, a rear side passivation layer maintaining its passivation properties after the firing process is needed. In recent years, a passivation layer consisting of aluminium oxide (Al_2O_3) deposited by atomic layer deposition (ALD) has shown to provide an outstanding level of surface passivation on crystalline silicon [1,2,3]. Implemented into lab-type PERC solar cells on *p*-type silicon very high independently confirmed efficiencies of 21.7% were achieved [4]. However, the standard (i.e. sequential) ALD process provides very low deposition rates < 2 nm/min. In order to implement the Al_2O_3 layer into an industrial process, higher deposition rates are required. Therefore, in this study we apply a new deposition technique using an inductively coupled plasma (ICP) plasma-enhanced chemical vapour deposition (PECVD) process. This process is developed in a laboratory-type tool at ISFH, as shown in the schematic drawing in Fig. 1. In this tool, a coil outside the vacuum chamber inductively excites the plasma using TMAl and O_2 as process gases. The main benefits of this deposition method are a very high plasma density allowing high deposition rates of up to 5 nm/s as well as low ion energies below 30 eV resulting in low surface damage and excellent passivation properties. In order to improve the firing stability, the Al_2O_3 layer is capped with a PECVD silicon nitride (SiN_y) layer [5]. In this work, we compare the passivation quality of ICP-AlO_x/SiN_y stacks and ALD-Al_2O_3/SiN_y stacks and their thermal stability. We implement both passivation systems into our PERC process [6] and demonstrate conversion efficiencies of up to 20.1% for large-area (156×156 mm^2) screen-printed PERC solar cells with ICP-AlO_x/SiN_y rear passivation.

2. Surface passivation quality

The symmetrical lifetime samples used in this study were fabricated on (100)-oriented 300 μm thick *p*-type float-zone (FZ) silicon wafers of 1.4 Ωcm resistivity with a size of 125×125 mm^2. The wafers were RCA-cleaned prior to surface passivation. Al_2O_3 films were deposited by plasma-assisted (PA) ALD in an Oxford Instruments FlexAL^{TM} reactor [7], or by ICP-PECVD using the CS 400P of Von Ardenne on both wafer surfaces. The SiN_y with a refractive index of n = 2.05 (at 632 nm) and a thickness of 100 nm was deposited by PECVD using a Roth & Rau SiNA system. The lifetime samples were characterized using the photoconductance decay method [8] (Sinton Instruments, WCT120 lifetime tester). Firing experiments were performed in an industrial infrared conveyor-belt furnace (Centrotherm Contact Firing Furnace DO 8.600-300) at a measured peak temperature of ~810°C for ~1 s, with a set temperature of 910°C. These are typical firing conditions for industrial screen-printed silicon solar cells.

Figure 2(a) shows the effective lifetime τ_{eff} as a function of Al_2O_3 layer thickness for single layers after
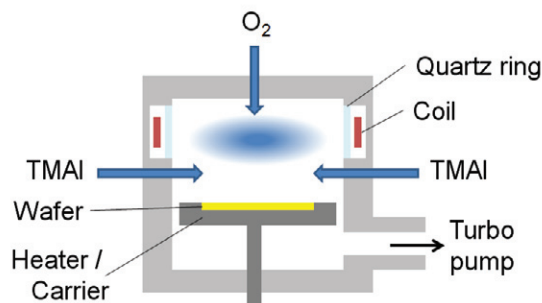

Fig. 1. Schematic of the laboratory-type ICP-AlO_x deposition chamber at ISFH. The plasma is inductively excited with a coil outside the vacuum chamber using TMAl and O_2 as process gases
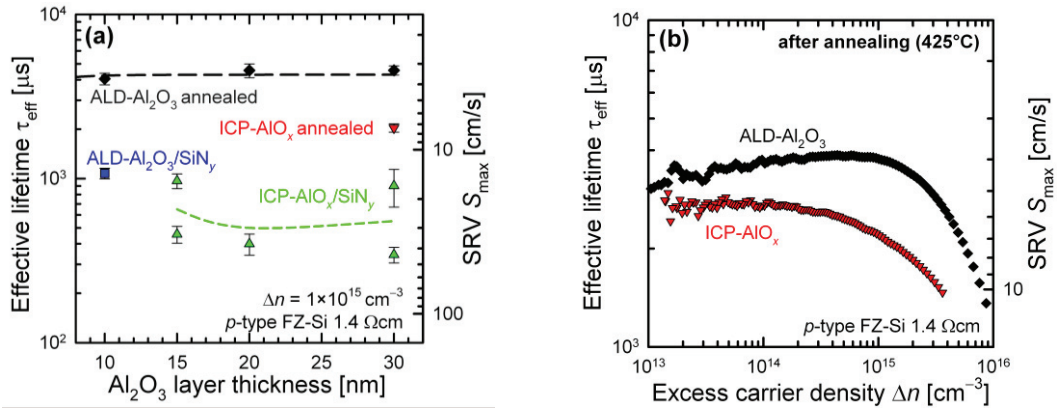
Fig. 2. (a) Effective lifetime τ_{eff} as a function of Al_2O_3 layer thickness for ICP-AlO$_x$ and ALD-Al$_2$O$_3$ single layers after annealing at 425°C and Al$_2$O$_3$/SiN$_y$ stacks. The stacks received no extra annealing. The lines are guides to the eye. (b) Effective lifetime τ_{eff} as a function of the excess carrier density Δn for 30 nm thick ICP-AlO$_x$ and ALD-Al$_2$O$_3$ layer after annealing at 425°C

annealing at 425°C and Al$_2$O$_3$/SiN$_y$ stacks with no extra annealing. After annealing at 425°C the samples with ICP-AlO$_x$ layers provide a very good surface passivation with lifetimes of 2 ms, which is almost as good as the excellent surface passivation of ALD-Al$_2$O$_3$ layers with lifetimes between 4 and 5 ms. In Fig. 2(a) it can be seen that the deposition of a SiN$_y$ layer on top of the non-annealed Al$_2$O$_3$ layer results in effective lifetimes of up to 1 ms for both Al$_2$O$_3$ layers, ICP and ALD. Figure 2(b) shows the effective lifetime τ_{eff} as a function of excess carrier density Δn for 30 nm thick ICP-AlO$_x$ and ALD-Al$_2$O$_3$ layers after annealing. Both Al$_2$O$_3$ layers provide a surface passivation with almost no injection level dependence in the injection range between 10^{13} and 10^{15} cm^{-3}.

The best lifetime results achieved are above the commonly used empirical expression for the intrinsic lifetime limit for crystalline silicon [9]. Therefore, in order to calculate a surface recombination velocity (SRV), we assume an infinitive bulk lifetime and use the expression $S_{max} = W/(2\tau_{eff})$. Using this expression, S_{max} values below 9 cm/s are calculated for annealed ICP-AlO$_x$ and below 5 cm/s for annealed ALD-Al$_2$O$_3$, showing the excellent passivation quality of both deposition techniques.

Figure 3(a) shows the effective lifetime τ_{eff} after firing as a function of Al$_2$O$_3$ layer thickness for
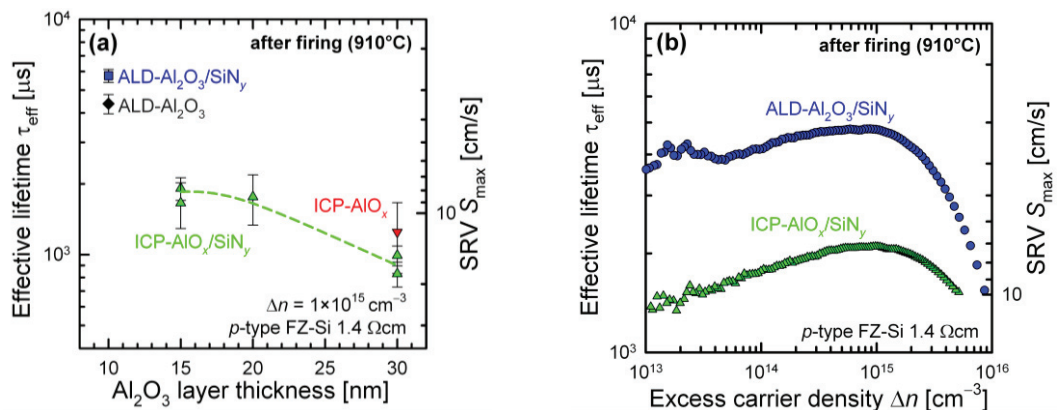

Fig. 3. (a) Effective lifetime τ_{eff} as a function of Al$_2$O$_3$ layer thickness for ICP-AlO$_x$ and ALD-Al$_2$O$_3$ after firing at a set peak temperature of 910°C. All Al$_2$O$_3$ layer systems received no annealing previous to the firing step. The lines are guides to the eye. (b) Effective lifetime τ_{eff} as a function of the excess carrier density Δn for Al$_2$O$_3$/SiN$_y$ stacks with a 20 nm thick ICP-AlO$_x$ layer and a 10 nm ALD-Al$_2$O$_3$ layer after firing

different layer systems. For the 30 nm thick ICP-AlO$_x$ layers almost no difference between the samples with and without SiN$_y$ capping layer can be observed. Both layer systems provide an effective lifetime of 1 ms after firing, corresponding to an S_{max} below 20 cm/s. The ICP-AlO$_x$/SiN$_y$ stacks with 15 nm and 20 nm AlO$_x$ layers provide a slightly higher lifetime between 1 and 2 ms, corresponding to an S_{max} below 12 cm/s. The single ALD-Al$_2$O$_3$ layers show no difference to the annealed samples in Fig. 2. The ALD-Al$_2$O$_3$/SiN$_y$ stacks, however, show an improvement and provide the highest effective lifetime of all samples with values up to 6 ms corresponding to an S_{max} value of 2.5 cm/s. The ICP-AlO$_x$ layer provide a surface passivation with a very good firing stability, however, the ALD-Al$_2$O$_3$ layers provide even lower S_{max} values. This difference in passivation quality between the ICP-AlO$_x$ layers and the ALD-Al$_2$O$_3$ layers is partly due to a slight blistering of the ICP-AlO$_x$ layers during the firing process. This blistering is mainly observed at samples with a 30 nm ICP-AlO$_x$ layer but can be observed for the samples with thinner AlO$_x$ layers as well. Figure 3(b) shows the effective lifetime τ_{eff} as a function of excess carrier density Δn for Al$_2$O$_3$/SiN$_y$ stacks with a 20 nm thick ICP-AlO$_x$ layer and a 10 nm ALD-Al$_2$O$_3$ layer after firing. It can be seen that the injection dependence does not change strongly compared to the annealed samples, S_{max} values below 12 cm/s can be measured over the injection range from 10^{13} to 10^{15} cm^{-3}. This should lead to an excellent cell performance also under weak light conditions.

3. Fixed charge density and interface state density

The reason for the outstanding passivation quality of the Al$_2$O$_3$ layers are the negative fixed charge density combined with a low interface state density. In order to measure the negative fixed charge density, the Corona charge analysis [10] was used. For the measurement of the interface state density the capacitance-voltage (C-V) analysis was used.

Figure 4(a) shows the upper limit of the surface recombination velocity S_{max} as a function of the Corona charge density Q_c for a 30 nm thick ICP-AlO$_x$ single layer and a 15 nm thick ALD-Al$_2$O$_3$ single layer after annealing at 425°C. It can be seen that both Al$_2$O$_3$ layers have almost the same negative fixed charge density with Q_f values of $-(4.5\pm1.0)\times10^{12}$ cm^{-2} for ICP-AlO$_x$ and $-(3.7\pm1.0)\times10^{12}$ cm^{-2} for ALD-Al$_2$O$_3$. Hence, it can be concluded that the negative fixed charge density is not the reason for the difference in passivation quality. Figure 4(b) shows the interface state density (D_{it}) as a function of
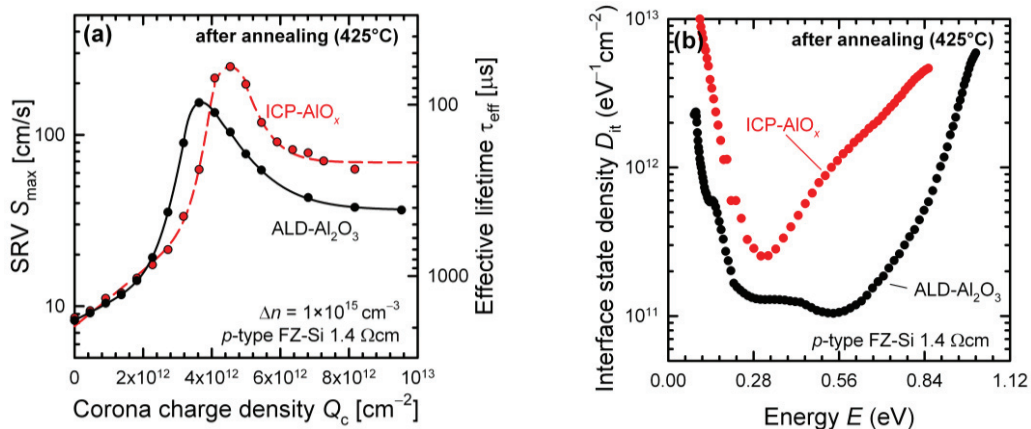

Fig. 4. (a) Surface recombination velocity as a function of Corona charge density. Shown are the values for a 30 nm thick ICP-AlO$_x$ layer and a 15 nm thick ALD-Al$_2$O$_3$ layer after annealing. The lines are guides to the eye. (b) Interface state density as a function of energetic position $E = E_t - E_v$. Shown are the values for a 30 nm thick ICP-AlO$_x$ layer and a 30 nm thick ALD-Al$_2$O$_3$ layer after annealing

energetic position $E = E_t - E_v$ above the silicon valence band edge E_v. Plotted are the values for a 30 nm thick ICP-AlO$_x$ layer and a 30 nm ALD-Al$_2$O$_3$ layer after annealing. The ICP-AlO$_x$ shows D_{it} values of $(11.0\pm4.0)\times10^{11}$ eV^{-1}cm^{-2} around midgap. This D_{it} is higher compared to the ALD-Al$_2$O$_3$ layer with low D_{it} values of $(1.3\pm0.4)\times10^{11}$ eV^{-1}cm^{-2}. The ICP-AlO$_x$ layer shows also a strong variation of D_{it} over the energetic position with D_{it} values almost as low as the ALD-Al$_2$O$_3$ layer around 0.28 eV. The higher D_{it} values around midgap explain the slightly lower passivation quality of the ICP-AlO$_x$ layers compared to the ALD-Al$_2$O$_3$ layers.

4. Application to PERC solar cells

We have implemented both stacks, the ICP-AlO$_x$/SiN$_y$ and the ALD-A$_2$O$_3$/SiN$_y$, into the ISFH PERC [6] process, with screen-printed front and rear contacts, a homogenously doped phosphorous emitter and laser contact openings (LCO) to form local Al BSF rear contacts using 156×156 mm^2 p-Type 2-3 Ωcm Cz silicon wafers. For the ICP-AlO$_x$/SiN$_y$ stack we used a 20 nm and a 30 nm thick AlO$_x$ layer and a 10 nm ALD-Al$_2$O$_3$ layer for the ALD-Al$_2$O$_3$/SiN$_y$ stack. Table 1 shows the results for the best cells. The PERC-

Tab. 1. Solar cell results for a PERC-type cell. Shown are the values for the best PERC-type cells with different passivation layers on the rear side

Rear side	Al$_2$O$_3$ layer thickness	V_{OC} [mV]	J_{SC} [mA/cm^2]	FF [%]	η [%]
ICP-AlO$_x$/SiN$_y$	30 nm	655	39.0	78.8	20.1*
ICP-AlO$_x$/SiN$_y$	20 nm	657	39.1	77.8	20.0*
ALD-Al$_2$O$_3$/SiN$_y$	10 nm	656	39.1	76.3	19.6

* Independently confirmed at Fraunhofer ISE CalLab.

type cell with a 30 nm ICP-AlO$_x$ layer achieves a high V_{OC} of 655 mV and a high J_{SC} of 39.0 mA/cm^2, which can be attributed to the excellent rear side passivation by the ICP-AlO$_x$/SiN$_y$ stack. This results in a high conversion efficiency of 20.1%. The cell with the 20 nm ICP-AlO$_x$ layer provides similar cell parameters. Compared to the cell with ALD-Al$_2$O$_3$/SiN$_y$ stack, the cell with ICP-AlO$_x$ layer performs slightly better due to a higher FF. However, the V_{OC} and J_{SC} values and internal quantum efficiency measurements show that the overall rear passivation is comparable for both deposition techniques. The high values of efficiencies measured for ICP-AlO$_x$/SiN$_y$ show for the first time that this deposition technique is very well suited for the implementation into industrial PERC cells.

5. Conclusion

In this contribution, we have shown that the AlO$_x$/SiN$_y$ stacks with AlO$_x$ layers deposited by ICP-PECVD provide an excellent passivation quality after firing with S_{max} values below 20 cm/s, what is almost as good as the Al$_2$O$_3$/SiN$_y$ stacks with Al$_2$O$_3$ layers deposited by PA-ALD featuring S_{max} below 3 cm/s. The main reason for the slightly higher S_{max} values compared to the ALD-Al$_2$O$_3$ reference layers, are higher D_{it} values of $(11.0\pm4.0)\times10^{11}$ eV^{-1}cm^{-2} around midgap compared to $(1.3\pm0.4)\times10^{11}$ eV^{-1}cm^{-2} for ALD-Al$_2$O$_3$, whereas the negative fixed charge density was found to be about -4×10^{12} cm^{-2} for both, ICP-AlO$_x$ and ALD-Al$_2$O$_3$. When implemented into an industrial-type PERC solar cell the ICP-AlO$_x$/SiN$_y$ stacks achieved outstanding cell efficiencies with values of up to 20.1%, compared to 19.6% for the ALD-Al$_2$O$_3$/SiN$_y$ passivated PERC-type cells. In conclusion, it can be said, that the ICP-PECVD deposition technique is very well suited as AlO$_x$-based rear passivation layer in industrial-type screen-printed PERC solar cells. The SINGULAR ICP-PECVD deposition tool of Singulus Technologies AG is

already using this technology for the deposition of SiN_x and SiO_x films. Currently, the integration of the $ICP\text{-}AlO_x$ process in combination with the SiN_y capping layer deposition is implemented.

Acknowledgements

References

[1] Agostinelli G, Delabie A, Vitanov P, Alexieva Z, Dekkers HFW, De Wolf S, Beaucarne G. Very low surface recombination velocities on *p*-type silicon wafers passivated with a dielectric with fixed negative charge. *Solar Energy Materials & Solar Cells* 2006; **90**:3438-3443

[2] Hoex B, Heil SBS, Langereis E, van de Sanden MCM, Kessels WMM. Ultralow surface recombination of c-Si substrates passivated by plasma-assisted atomic layer deposited Al_2O_3. *Apllied Physics Letters* 2006; **89**:042112

[3] Dingemans G, Seguin R, Engelhart P, van de Sanden MCM, Kessels WMM. Silicon surface passivation by ultrathin Al_2O_3 films synthesized by thermal and plasma atomic layer deposition. *Physica Status Solidi Rapid Research Letters* 2010; **4**:10-12

[4] Zielke D, Petermann JH, Werner F, Veith B, Brendel R, Schmidt J. Contact passivation in silicon solar cells using atomic-layer-deposited aluminum oxide layers. *Physica Status Solidi Rapid Research Letters* 2011; **5**:298-300

[5] Schmidt J, Veith B, Brendel R. Effective surface passivation of crystalline silicon using ultrathin Al_2O_3 films and Al_2O_3/SiN_x stacks. *Physica Status Solidi Rapid Research Letters* 2009; **3**:287-289

[6] Dullweber T, Gatz S, Hannebauer H, Falcon T, Hesse R, Schmidt J, Brendel R. et al. Towards 20% efficient large-area screen-printed rear-passivated silicon solar cells. *Prog. Photovolt: Res. Appl.* 2011; doi: 10.1002/pip.1198

[7] Heil SBS, van Hemmen JL, Hodson CJ, Singh N, Klootwijk JH, Roozeboom F et al. Deposition of TiN and HfO_2 in a commercial 200 mm remote plasma atomic layer deposition reactor. *Journal of Vacuum Technology A* 2007; **25**:1357-1366

[8] Kane DE, Swanson RM. Measurement of the emitter saturation current by a contactless photoconductivity decay method. *Proceedings of the 18th IEEE Photovoltaic Specialists Conference, Las Vegas, USA*, 1985, pp. 578-583.

[9] Kerr MJ, Cuevas A. General parameterization of Auger recombination in crystalline silicon. *Journal of Applied Physics* 2002; **91**:2473- 2480

[10] Dauwe S, Schmidt J, Metz A, Hezel R. Fixed charge density in silicon nitride films on crystalline silicon surfaces under illumination. *Proceedings of the 29th IEEE Photovoltaic Specialists Conference, New Orleans, USA*, 2002, pp. 162-165.